Available online at www.sciencedirect.com
ScienceDirect
Journal of Nuclear Materials 362 (2007) 480–484
journal of nuclear materials
www.elsevier.com/locate/jnucmat

# Behaviour of simplified nuclear waste glasses under gold ions implantation: A microluminescence study

J. de Bonfils [a,*], G. Panczer [a], D. de Ligny [a], S. Peuget [b], B. Champagnon [a]

[a] *Université Claude Bernard Lyon 1, Laboratoire de Physico-Chimie des Matériaux Luminescents, UMR 5620, 12 rue Ampère, 69622 Villeurbanne, France*
[b] *Commissariat à l'Energie Atomique, CEA Marcoule, DEN/DTCD, BP 17171, 30207 Bagnols-sur-Cèze cedex, France*

---

## Abstract

Simplified nuclear borosilicate glasses doped with rare-earth elements were irradiated by gold ions. Thanks to fluorescence line narrowing spectroscopy (selective excitated photoluminescence), two major $Eu^{3+}$ sites distributions were identified in the case of pre-irradiated samples due to the splitting of the $^5D_0 \rightarrow {}^7F_1$ transition triplet. Evolution of europium ion environments under irradiation in these glasses was studied by non-selective microluminescence at room temperature. As well, spectroscopic studies demonstrated strong broadening in the distribution of the rare-earth environment for increasing irradiation doses. Determination of the luminescence asymmetric ratio allowed us to conclude that the symmetry of the sites is lowered by high energy nuclear deposits. Environment modifications under irradiation are attributed to a site distribution enlargement within the same two site distributions, a silicate and a borate one, and to lower symmetry mean sites.

*PACS:* 78.60.−b; 32.50.+d; 61.80.−x

---

## 1. Introduction

In France, the high activity wastes, stemming from the reprocessing of the irradiated nuclear fuels, are confined in a borosilicate glass called R7T7. The prediction of the long-term behaviour of this glass is then essential. For that purpose, simplified glasses are irradiated with multienergy Au ions to simulate the consequences of alpha decay.

Several Raman studies have shown that the medium range order structure is very sensitive to irradiation. For instance the Si–O–Si bending band located at 495 $cm^{-1}$ shifts for different glasses under neutrons [1], electrons [2] or heavy ions irradiations [3]. For increasing Au implantation doses, a progressive shift is observed towards the high wavenumbers of the vibrational band located at 495 $cm^{-1}$, corresponding to an average Si–O–Si bond angle reduction as well as a reduction in the rings average size [2]. This angle decrease is characteristic of a densification of the glassy network. Despite this medium range densification, nothing

---

[*] Corresponding author. Tel.: +33 4 72 44 82 21; fax: +33 4 72 44 84 32.
*E-mail address:* jdebonfils@pcml.univ-lyon1.fr (J. de Bonfils).

0022-3115/$ - see front matter © 2007 Elsevier B.V. All rights reserved.
doi:10.1016/j.jnucmat.2007.01.101

Table 1
Glasses composition (fractions of oxides are in molar percent)

| | $SiO_2$ | $Na_2O$ | $B_2O_3$ | $Al_2O_3$ | CaO | $ZrO_2$ | $Eu_2O_3$ |
|---|---|---|---|---|---|---|---|
| CJ1 $Eu^{3+}$ | 67.09 | 14.08 | 17.83 | – | – | – | 1.00 |
| CJ3 $Eu^{3+}$ | 60.55 | 12.72 | 16.13 | 3.85 | 5.75 | – | 1.00 |
| CJ7 $Eu^{3+}$ | 63.13 | 13.26 | 16.81 | 4.01 | – | 1.79 | 1.00 |

is known yet on the rare-earth elements local environment which can be related to glass aging.

In order to understand the structure in a small range order in nuclear waste glasses, simplified glasses were doped with $Eu^{3+}$ (Table 1). As a matter of fact, europium has the same structural properties than minor actinides, especially americium which is an electronic analogue of europium, with respect to the vitreous matrix. Moreover, thanks to its spectroscopic properties, $Eu^{3+}$ can be used as a luminescent structural probe [4,5]. This setting-up allows to simulate the actinides radiations in the active glass.

## 2. Experimental

### 2.1. Samples preparation

Samples were prepared in a Pt crucible by fusion of a mixture of oxide around 1775 K during 3 h (see Table 1 for compositions). Annealing was realized in hot graphite moulds around 865 K during 1 h. Glasses were cut in 2–3 mm thick sections and polished on both sides. Alpha decay damages were simulated by external irradiation of non-radioactive glasses by gold ions [6]. Energy and fluence were selected to investigate the effects of electronic and nuclear processes over dose ranges comparable to those obtained in actinide-doped glass. Au irradiations were carried out in the centre of Nuclear Spectroscopy and Mass Spectroscopy (CSNSM, Paris XI). Samples were irradiated with multienergy Au ions to obtain a constant nuclear deposited energy along a 2 μm thick layer at the glass surface (Table 2). Amounts of irradiation have been chosen to simulate nuclear deposited energy corresponding to α-fluences between $8 \times 10^{16}$ and $1.9 \times 10^{19}$ alpha disintegrations per gram of glass.

### 2.2. Experimental setup

Fluorescence Line Narrowing spectra, FLN, were recorded within an excitation ranged from 570 nm to 580 nm by 0.5 nm step. In order to minimize the background due to the thermal lattice vibrations, samples were cooled at liquid nitrogen temperature (77 K). Such selective excitations were realized with a pulsed dyed laser (LUMONICS Hyper-Dye 300 with Rhodamine 590) pumped by an Excimer laser (LUMONICS Excimer-500 at 308 nm, pulse duration: 10 ns with a 0.1 $cm^{-1}$ spectral width, energy pulse: around 30 mJ). Luminescence signal was collected through a ×100 Olympus objective and then sent into a 1200 grooves per mm grating (ORIEL Multispec) thanks to an optical fibre. Data were monitored with an intensified CCD (ORIEL Instaspec V) cooled by Peltier effect. This method consists in a selective excitation in the range of the $^5D_0 \rightarrow {}^7F_0$ transition. For each excitation wavelength, only a few specific set of $Eu^{3+}$ sites (i.e. the same local environment) are sensitive to the excitation and produce a luminescence signal specific to their own environment. By selecting precisely the excitation, it becomes possible to collect the signal of all the different sets of sites separately.

Table 2
Irradiation conditions

| | Ion fluence ($cm^{-2}$) | $E$ (MeV) (cumulative values) | Nuclear energy (keV $cm^{-3}$) | Electronic energy (keV $cm^{-3}$) |
|---|---|---|---|---|
| F2 | $6.1 \times 10^{11}$ | 1 | $5.0 \times 10^{19}$ | $1.7 \times 10^{20}$ |
| | $1.8 \times 10^{12}$ | 3.5 | | |
| | $4.2 \times 10^{12}$ | 7 | | |
| F4 | $2.4 \times 10^{12}$ | 1 | $2.0 \times 10^{20}$ | $6.8 \times 10^{20}$ |
| | $7.3 \times 10^{12}$ | 3.5 | | |
| | $1.7 \times 10^{13}$ | 7 | | |
| F6 | $4.6 \times 10^{13}$ | 1 | $3.8 \times 10^{21}$ | $1.3 \times 10^{22}$ |
| | $1.4 \times 10^{14}$ | 3.5 | | |
| | $3.2 \times 10^{14}$ | 7 | | |

Non-selective microluminescence spectra have been recorded at room temperature on a microspectrometer Renishaw RM1000 with a 1800 grooves per mm grating. The 514 nm Ar laser (Spectra Physic – 75 mW) was focused on the sample through a ×100 Olympus objective. The luminescence signal was collected, through the same objective and a 10 μm slit, in a CCD cooled by Peltier effect. By this way, one can work in a confocal mode which enables us to work in the 2 μm thick irradiated layer [3]. The spectra are built with 20 s integration time for each point.

For the two analysis methods, all the data were analysed with GRAMS software. Deconvolutions of FLN and microluminescence spectra and the areas calculation were processed with the Levenberg–Marquadt method [7] coupled with Gaussian functions.

## 3. Results and discussion

### 3.1. Fluorescence line narrowing spectroscopy

Fluorescence line narrowing spectra were obtained by tuning the dye laser over the energy range of the $^5D_0 \rightarrow {}^7F_0$ region. The Pucker's procedure [8] is adopted and the well defined $^5D_0 \rightarrow {}^7F_1$ transition in which the Stark sub levels are split into three components $(2J+1)$, is then studied. The $^5D_0 \rightarrow {}^7F_2$ transition could be also used as reported by Brecher and Riseberg [9] but unfortunately showed a lower resolution. For the following discussion, only the $^7F_1$ Stark sub-levels are considered.

Fig. 1 shows the site-selective emission spectrum of the $^5D_0 \rightarrow {}^7F_1$ transition at 77 K as a function of the energy for a 577.5 nm excitation. The emission spectra were deconvoluted into six Gaussian components which is an evidence for two major sites distributions in this glass. Same results are obtained for CJ3 and CJ7 samples. The assignment of Stark components $(\varepsilon_0, \varepsilon_-, \varepsilon_+)$ is discussed in the work of Pucker et al. [8]. For each excitation wavelength, the six Stark components positions are recorded.

### 3.2. The ligand field parameter $B_2$: calculation and use

The $C_{2v}$ symmetry is retained for the ligand-field calculation because it is the highest symmetry which allows full splitting of $^7F_1$ and $^7F_2$ states of $Eu^{3+}$. To compare our results to data in the literature, the definition of an average ligand-field parameter [10] is used. This parameter, called $B_2$, is related to the crystal field parameters $B_{20}$ and $B_{22}$ (Eq. (1)).

$$\begin{aligned} B_{20} &= 5 \times \left(E(\varepsilon_0) - E({}^7F_1)\right), \\ B_{22} &= \pm\frac{10}{\sqrt{6}}E(\varepsilon_\pm) \mp \frac{5\sqrt{6}}{2}E({}^7F_1) \pm \frac{5}{\sqrt{6}}E(\varepsilon_0), \qquad (1) \\ B_2 &= \sqrt{(B_{20})^2 + 2(B_{22})^2}. \end{aligned}$$

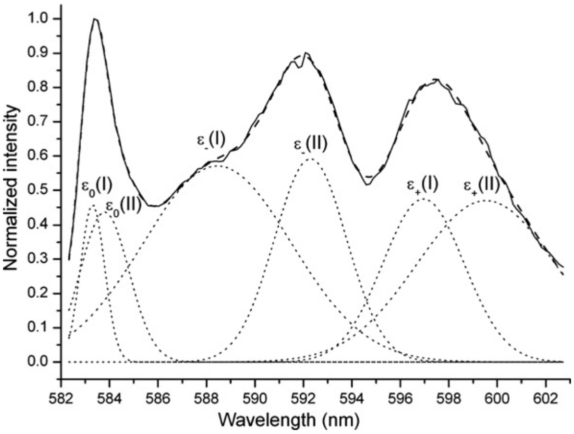

Fig. 1. $Eu^{3+}$ emission spectrum of the $^5D_0 \rightarrow {}^7F_0$ in CJ1. The spectrum was deconvoluted with a six Gaussian-profile components fit and can be related to two triplet identified as I and II. These triplets corresponding to two major distribution $Eu^{3+}$ sites. Experiment was realized at 77 K under a 577.5 nm laser excitation at 77 K. Solid line is experimental data. Deconvolution curves are in dotted lines. Result of the fit is in dashed line.

$E(^7F_1)$ is the barycentre of the $^7F_1$ triplet. $B_2$ is expressed as a function of $B_{20}$ and $B_{22}$. $E(\varepsilon_0)$ and $E(\varepsilon_\pm)$ are the positions of the stark sub-levels. $B_2$ values have been calculated for the two triplets of each spectrum and thus for all the three non-irradiated samples. The $B_2$ parameter is then compared with values issues from the literature. In the case of CJ1, the two site distributions have been identified as follows (Fig. 2): the first environment is a silicate-rich one and the second is a borate-rich environment [5]. For the 5-oxides glasses, CJ3 and CJ7, a silicate-rich environment and a mixed aluminate–borate-rich one are found. This result is consistent with recent work using Fluorescence Line Narrowing [4], where authors make the hypothesis of a two sites distribution for europium in the French non-active nuclear glass (R7T7).

### 3.3. Irradiation effects

Irradiation effects must be observed only within the two first micrometers from the surface. Such a thin probe can be only realized by confocal microluminescence spectroscopy. Emission spectra of CJ1:$Eu^{3+}$ under Au irradiation were recorded at room temperature with a 514 nm laser in the 560–640 nm range (Fig. 3). Transitions $^5D_0 \rightarrow {}^7F_j$ $(j = 0–2)$ of $Eu^{+3}$ were observed. The $^5D_0 \rightarrow {}^7F_0$ emission band is centred at 577.3 nm for the non-irradiated sample. The full-width at half maximum

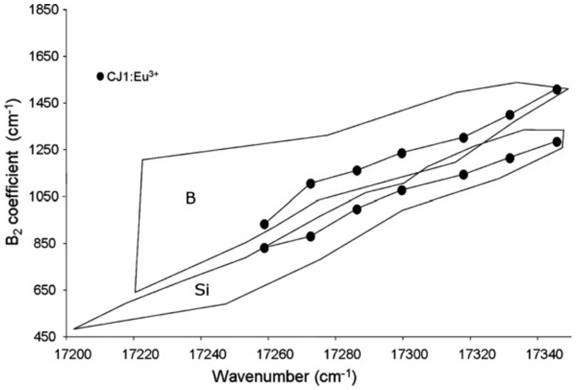

Fig. 2. Evolution of the ligand field parameter $B_2$ versus excitation energy in the CJ1:Eu$^{3+}$ glass (this work). $B_2$ domains for various borate and silicate environments are delimited ([9,11]). Each distribution site can be identified to a silicate rich or a borate rich environment.

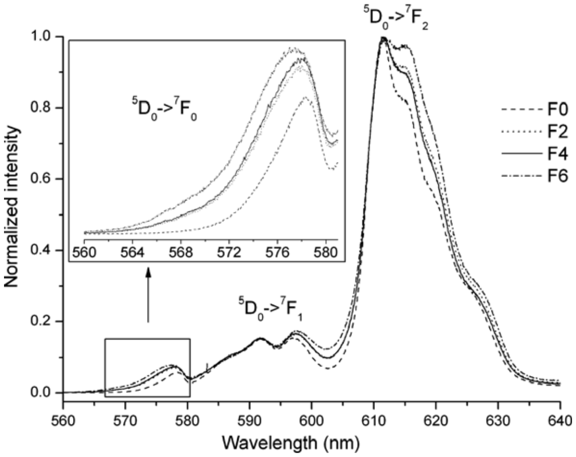

Fig. 3. Effect of gold ions fluences on the evolution of CJ1:Eu$^{3+}$ emission spectra. Index of the emission bands are mentioned above them. The value at F0 corresponds to the non-irradiated sample. Spectra were collected under a 514 nm continuous excitation at room temperature in confocal mode.

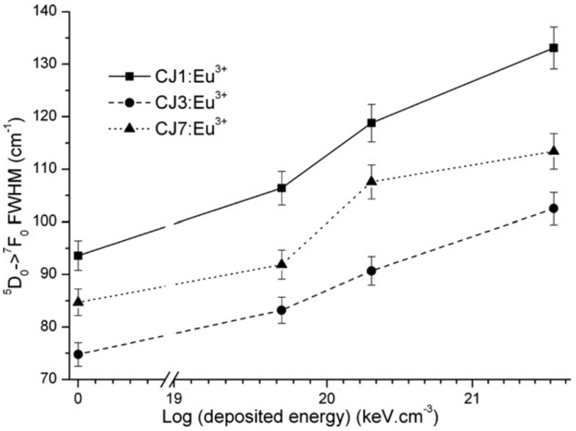

Fig. 4. Effect of gold ions fluences on the evolution of the full width at half maximum (FWHM) of the $^5D_0 \rightarrow {^7F_0}$ emission band for CJ1, 3, 7:Eu$^{3+}$. The same trend is observed for all samples. FWHM values were obtained from emission spectra recorded at room temperature under a 514 continuous excitation in confocal mode. Non-irradiated samples were arbitrary positioned at 0 keV cm$^{-3}$.

(FWHM) is 74, 85 and 93 cm$^{-1}$, respectively to CJ3:Eu$^{3+}$, CJ7:Eu$^{3+}$ and CJ1:Eu$^{3+}$ at F0 (Fig. 4). These values are in good agreement with values obtain previously on Na borosilicate glass [8,11] (80–94 cm$^{-1}$) in regards with decreasing SiO$_2$ amounts. According to Boyer et al. [12], the crystal field strength and the Eu–O distance decrease with increasing silica content which is consistent with our values (SiO$_2$ content: CJ1 > CJ7 > CJ3). The $^5D_0 \rightarrow {^7F_2}$ emission band is also modified under irradiation. Considering only the $^5D_0 \rightarrow {^7F_0}$ transition, the FWHM increases with irradiation doses: values range from 93 cm$^{-1}$ (Fig. 4) for non-irradiated glass to 133 cm$^{-1}$ for the maximum dose in the case of CJ1:Eu$^{3+}$. Same behaviour is observed for the others Eu$^{3+}$ doped glasses (Fig. 4). The asymmetric ratio, As, is defined as the ratio of the intensity of the $^5D_0 \rightarrow {^7F_2}$ by the intensity of the $^5D_0 \rightarrow {^7F_1}$. The electric dipole transition $^5D_0 \rightarrow {^7F_2}$ is a hypersensitive transition, i.e. sensitive to Eu$^{3+}$ second neighbours. This transition intensity increases with the ligands valence or with decreasing site symmetry [13]. On the contrary, the intensity $^5D_0 \rightarrow {^7F_1}$ magnetic transition is less sensitive to Eu$^{3+}$ environment and is chosen as reference. Accordingly the asymmetric ratio roughly increases for increasing irradiation doses (Table 3). This evolution is characteristic of a site symmetry reduction [13]. The site distribution for Eu$^{3+}$ is then broader for high doses and the mean site environment has evolved to lower symmetry.

Table 3
Asymmetric ratios (–) of Eu$^{3+}$ doped glasses under different conditions of irradiations (non-irradiated sample is mentioned as 'F0')

| Asymmetric ratios (–) | CJ1:Eu$^{3+}$ | CJ3:Eu$^{3+}$ | CJ7:Eu$^{3+}$ |
|---|---|---|---|
| F0 | 5.72 | 5.73 | 5.73 |
| F2 | 5.89 | 5.88 | 6.04 |
| F4 | 5.76 | 5.66 | 6.46 |
| F6 | 6.25 | 6.51 | 6.92 |

## 4. Conclusion

This work demonstrated that $Eu^{3+}$ is a useful luminescent structural probe to follow the aging of nuclear waste glasses under irradiations. Using ligand field parameters obtained from spectroscopy measurements, it was possible to identify two major $Eu^{3+}$ site distributions in non-irradiated samples. The first environment is clearly a silicate-rich one and the second is either a borate-rich (CJ1), either an alumino-borate one (CJ3 and CJ7). This result confirms previous works [4,5] on the French nuclear glass. Moreover, $Eu^{3+}$ short range environment is sensitive to glass composition depending mostly of $SiO_2$ content. The asymmetric ratio, As, informed us that $Eu^{3+}$ environment is drastically modified under Au implantations. Furthermore, the observed site symmetry decrease implies that $Eu^{3+}$ evolves to more complex environments during gold implantation. Currently, in Fluorescence Line Narrowing experiment, it is not possible to work in confocal mode due to experiment restriction (spatial resolution). Nevertheless, a modification is planed to provide accurate sites identification in the 2 μm irradiated layers.

## Acknowledgement

This work was carried out in the Common Center for Optical Microspectrometry (CECOMO), Université Claude Bernard Lyon 1.

## References

[1] J.B. Bates, R.W. Hendricks, L.B. Schaffer, J. Chem. Phys. 61 (1974) 4163.
[2] B. Boizot, S. Agnelo, B. Reynard, R. Boscaino, G. Petite, J. Non-Cryst. Solids 325 (2003) 22.
[3] S. Peuget, J. de Bonfils, G. Panczer, D. de Ligny, P.-Y. Noël, A. Chenet, J. Non-Cryst. Solids, submitted for publication.
[4] N. Ollier, G. Panczer, B. Champagnon, G. Boulon, P. Jollivet, J. Lumin. 94&95 (2001) 197.
[5] F. Thévenet, G. Panczer, P. Jollivet, B. Champagnon, J. Non-Cryst. Solids 351 (2005) 673.
[6] S. Peuget, P.-Y. Noël, J.-L. Loubet, S. Pavan, P. Nivet, A. Chenet, Nucl. Instrum. and Meth. B 246 (2006) 379.
[7] D. Marquardt, J. Soc. Ind. Appl. Math. 11 (1963) 431.
[8] G. Pucker, K. Gatterer, H.P. Bettinelli, M. Ferrari, Phys. Rev. B 53 (1996) 6225.
[9] C. Brecher, L.A. Riseberg, Phys. Rev. B 13 (1976) 81.
[10] R. Balda, J. Fernandez, H. Eilers, W.M. Yen, J. Lumin. 59 (1994) 81.
[11] C. Brecher, L.A. Riseberg, J. Non-Cryst. Solids 40 (1980) 469.
[12] L. Boyer, B. Piriou, J. Carpena, J.L. Lecout, J. Alloys Compd. 311 (2000) 143.
[13] K. Gatterer, G. Pucker, H.P. Fritzer, Phys. Chem. Glasses 38 (1997) 293.